AJNR

Bone-Subtraction CT Angiography: Evaluation of Two Different Fully Automated Image-Registration Procedures for Interscan Motion Compensation

M.M. Lell, H. Ditt, C. Panknin, J.W. Sayre, S.G. Ruehm, E. Klotz, B.F. Tomandl and J.P. Villablanca

AJNR Am J Neuroradiol 2007, 28 (7) 1362-1368
doi: https://doi.org/10.3174/ajnr.A0558
http://www.ajnr.org/content/28/7/1362

ORIGINAL RESEARCH

Bone-Subtraction CT Angiography: Evaluation of Two Different Fully Automated Image-Registration Procedures for Interscan Motion Compensation

M.M. Lell
H. Ditt
C. Panknin
J.W. Sayre
S.G. Ruehm
E. Klotz
B.F. Tomandl
J.P. Villablanca

BACKGROUND AND PURPOSE: Bone-subtraction techniques have been shown to enhance CT angiography (CTA) interpretation, but motion can lead to incomplete bone removal. The aim of this study was to evaluate 2 novel registration techniques to compensate for patient motion.

MATERIALS AND METHODS: Fifty-four patients underwent bone-subtraction CTA (BSCTA) for the evaluation of the neck vessels with 64-section CT. We tested 3 different registration procedures: pure rigid registration (BSCTA), slab-based registration (SB-BSCTA), and a partially rigid registration (PR-BSCTA) approach. Subtraction quality for the assessment of different vascular segments was evaluated by 2 examiners in a blinded fashion. The Cohen kappa test was applied for interobserver variability, and the Wilcoxon signed rank test, for differences between the procedures. Motion between the corresponding datasets was measured and plotted against image-quality scores.

RESULTS: Algorithms with motion compensation revealed higher image-quality scores (SB-BSCTA, mean 4.31; PR-BSCTA, mean 4.43) than pure rigid registration (BSCTA, mean 3.88). PR-BSCTA was rated superior to SB-BSCTA for the evaluation of the cervical internal and external carotid arteries ($P <$ .001), whereas there was no significant difference for the other vessels (P = .157–.655). Both algorithms were clearly superior to pure rigid registration for all vessels except the basilar and ophthalmic artery. Interobserver agreement was high (κ = 0.46–0.98).

CONCLUSION: Bone-subtraction algorithms with motion compensation provided higher image-quality scores than pure rigid registration methods, especially in cases with complex motion. PR-BSCTA was rated superior to SB-BSCTA in the visualization of the internal and external carotid arteries.

CT angiography (CTA) has been demonstrated to be an accurate and cost-effective alternative to conventional angiography and MR angiography in a variety of clinical settings.[1-9] The resulting datasets are usually visualized by means of maximum intensity projection (MIP) or volume rendering. A limitation of rendered CTA is that vessels surrounded by bone and calcification can be obscured. To eliminate voxels representing bone or calcification in the final image and prevent them from possibly obscuring the visualization of vessels, one may apply bone-subtraction techniques. Bone-subtraction CTA (BSCTA), using a (low-dose) nonenhanced scan to create a bone model, which then is subtracted from the CTA data,[10-13] has proved to be a robust method, which can be fully automated, requiring no user interaction. This technique has been shown to be beneficial in a variety of clinical settings.[10,12-15]

A limitation of this method is that complex patient motion between the 2 scans can confound the subtraction process. The skull defines a nondeformable compartment that can generally be registered sufficiently even in the presence of severe interscan motion. In contrast, the independent mobility of the cervical bones, mandible, hyoid, or larynx cannot be compensated by using global rigid registration techniques and will, therefore, result in incomplete removal. The first step to reduce patient motion is to educate the patient about the importance of remaining still during the scanning and to use a comfortable restraining device. If motion cannot be sufficiently prevented by these means, special registration algorithms must be applied to obtain diagnostic image quality.

In this article, we compare 2 different approaches to minimize bone remnants in the final BSCTA images of the neck vessels: a slab-based segmentation algorithm and a partially rigid segmentation algorithm.

Received October 23, 2006; accepted after revision December 4.

From the Department of Radiological Sciences (M.M.L., C.P., J.W.S., S.G.R., J.P.V.), David Geffen School of Medicine at the University of California, Los Angeles, Calif; Siemens Medical Solutions (H.D., C.P., E.K.), Forchheim, Germany; the Department of Biostatistics (J.W.S.), the University of California, Los Angeles School of Public Health, Los Angeles, Calif; and the Department of Neuroradiology (B.F.T.), Klinikum Bremen-Mitte, Bremen, Germany.

Please address correspondence to Michael Lell, MD, Department of Radiological Sciences, David Geffen School of Medicine at UCLA, Peter V. Ueberroth Bldg, Suite 3371, 10945 LeConte Ave, Los Angeles, CA 90095; e-mail: Michael.Lell@idr.med.uni-erlangen.de

DOI 10.3174/ajnr.A0558

Materials and Methods

We consecutively enrolled 54 patients who were scheduled for CTA of the head and neck region. Written informed consent was obtained from each individual or their legal representatives after the nature of the procedure had been fully explained; the study was conducted in accordance with the institutional review board guidelines. Patients with contrast allergy and renal insufficiency were excluded from the study.

The patient population was composed of 2 groups: 1) patients with symptomatic atherosclerotic disease who underwent an additional low-dose nonenhanced CT scanning (NECT) for subtraction purposes and 2) patients with cancer of the oral cavity/oropharynx who required CTA for surgical planning of reconstructive surgery. In the latter group, a late-phase venous CT scanning (LVCT) indicated for tumor staging was used as a substitute for the NECT to create a bone mask. The oncology population was included in the study because of the possibility of greater motion in this group, for they were experiencing a longer delay between the 2 scannings (CTA-LVCT).

CTA

The study was performed by using a 64-section CT system (Sensation 64; Siemens Medical Solutions, Forchheim, Germany). Patients were positioned supine with the head comfortably fixed in a standard head holder device and were instructed to breathe normally and to avoid

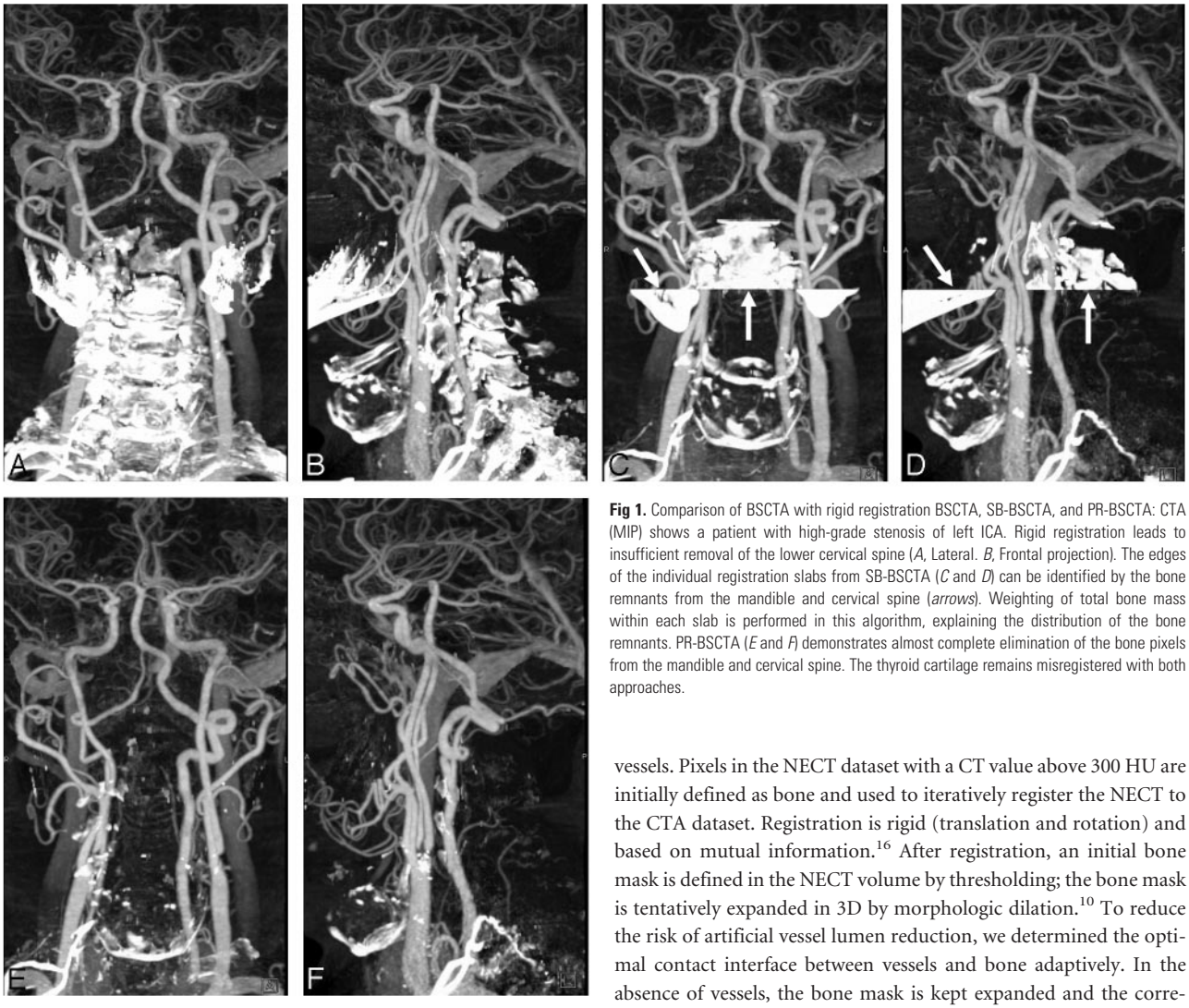

Fig 1. Comparison of BSCTA with rigid registration BSCTA, SB-BSCTA, and PR-BSCTA: CTA (MIP) shows a patient with high-grade stenosis of left ICA. Rigid registration leads to insufficient removal of the lower cervical spine (*A*, Lateral. *B*, Frontal projection). The edges of the individual registration slabs from SB-BSCTA (*C* and *D*) can be identified by the bone remnants from the mandible and cervical spine (*arrows*). Weighting of total bone mass within each slab is performed in this algorithm, explaining the distribution of the bone remnants. PR-BSCTA (*E* and *F*) demonstrates almost complete elimination of the bone pixels from the mandible and cervical spine. The thyroid cartilage remains misregistered with both approaches.

swallowing during and between the scannings. Circulation time was measured with the test-bolus technique (10-mL contrast material, region of interest for measurements in the common carotid artery) in all patients. The nonenhanced low-dose scanning was performed after the test-bolus evaluation. The CTA scanning with the patient-specific scanning delay followed subsequently. Scanner settings were the following: 120 kV, 50 effective (eff) mAs (NECT), 180 eff mAs (CTA), 0.33 rotation time, pitch of 0.9, 64 × 0.6 mm section acquisition, 0.75-mm reconstructed section thickness, 0.5-mm reconstruction increment, 512 × 512 matrix, adapted FOV (130–180 mm) by using a soft-tissue kernel (H 20). Contrast material was injected with a dual-head power injector. The average amount was 80 mL, the flow rate was 5 mL/s, and a saline bolus (50-mL sodium chloride 0.9%) followed the contrast injection.

Bone Subtraction

Data were transferred to a workstation (Leonardo; Siemens Medical Solutions) equipped with a prototype software tool for bone-subtraction CTA that allows selection of different registration modes (rigid registration [BSCTA], slab-based rigid registration [SB-BSCTA], and partial rigid registration [PR-BSCTA]). The BSCTA process includes the following steps: After both datasets are loaded, the algorithm selectively eliminates bone from the CTA dataset automatically without user interaction, retaining both soft-tissue and contrast-enhanced vessels. Pixels in the NECT dataset with a CT value above 300 HU are initially defined as bone and used to iteratively register the NECT to the CTA dataset. Registration is rigid (translation and rotation) and based on mutual information.[16] After registration, an initial bone mask is defined in the NECT volume by thresholding; the bone mask is tentatively expanded in 3D by morphologic dilation.[10] To reduce the risk of artificial vessel lumen reduction, we determined the optimal contact interface between vessels and bone adaptively. In the absence of vessels, the bone mask is kept expanded and the corresponding voxels are set to a CT value of −1024 HU; in areas of bone-vessel contact, the corresponding NECT voxels are locally subtracted.[10]

As an extension to this registration step, the prototype software can perform 2 further procedures to compensate for motion between the 2 scannings: The first algorithm uses an SB-BSCTA and is similar to a commercially available tool (NeuroDSA; Siemens Medical Solutions) in which the volume is subdivided into slabs of approximately 1.5 cm in height along the z-axis, and repeated registration for each slab is performed. The second algorithm applies partial rigid registration step (PR-BSCTA). This includes the following steps: 1) single rigid registrations step of the scans based on mutual information, 2) calculation of misregistration areas, and 3) iterative rigid registration on areas with significant misregistration.[17]

Image Evaluation

Before image evaluation, datasets were anonymized and presented to the examiners in random order without information regarding registration technique or clinical data. The 3 subtraction techniques were examined during different reading sessions, separated from each other by approximately 2 weeks to minimize recall bias. We have chosen the MIP technique for evaluation because it is a widely used postprocessing technique and bone remnants are highlighted, thus facilitating the assessment of the subtraction results.

The assessment of vascular segments (common carotid artery [CCA],

Table 1: Summary of quality scores for angiograms processed with pure rigid BSCTA, SB-BSCTA, and PR-BSCTA

	BSCTA				SB-BSCTA				PR-BSCTA			
Vessel	Mean	±SD	Med	Range	Mean	±SD	Med	Range	Mean	±SD	Med	Range
CCA												
Reader 1	3.50	1.1	4	1–5	4.41	0.65	4.5	3–5	4.33	0.64	4	3–5
Reader 2	3.50	1.1	4	1–5	4.24	0.66	4	3–5	4.37	0.59	4	3–5
ICA												
Reader 1	3.48	0.81	3.5	2–5	3.96	0.79	4	2–5	4.26	0.64	4	3–5
Reader 2	3.48	0.81	3.5	2–5	3.89	0.74	4	2–5	4.20	0.65	4	3–5
ECA												
Reader 1	3.43	0.83	3	2–5	3.91	0.75	4	3–5	4.30	0.60	4	3–5
Reader 2	3.46	0.88	3.5	2–5	3.78	0.71	4	3–5	4.24	0.61	4	3–5
PC-ICA												
Reader 1	4.65	0.51	5	3–5	4.92	0.27	5	4–5	4.87	0.34	5	4–5
Reader 2	4.61	0.56	5	3–5	4.81	0.39	5	4–5	4.79	0.41	5	4–5
VA												
Reader 1	2.50	1.1	3	1–5	3.50	0.83	4	2–5	3.50	0.88	4	1–5
Reader 2	2.52	1.1	3	1–5	3.61	0.70	4	2–5	3.74	0.75	4	2–5
BA												
Reader 1	4.90	0.3	5	4–5	4.98	0.14	5	4–5	4.96	0.19	5	4–5
Reader 2	4.88	0.33	5	4–5	4.92	0.27	5	4–5	4.96	0.19	5	4–5
OA												
Reader 1	4.80	0.68	5	1–5	4.83	0.67	5	1–5	4.83	0.67	5	1–5
Reader 2	4.60	0.92	5	1–5	4.63	0.91	5	1–5	4.70	0.81	5	1–5

Note:—Med indicates median.

Fig 2. CTA (MIP, frontal [*A* and *C*] and lateral [*B* and *D*] views) shows a patient with atherosclerotic disease at the carotid bifurcation and siphon. Correct registration and successful removal of the calcified plaque at the carotid siphon is obtained with both registration techniques. Pulsation leads to incomplete removal at the left carotid bifurcation, more pronounced with SB-BSCTA (*A* and *B*), whereas removal of the calcifications at the right carotid bifurcation is almost perfect with both methods. Removal of the lower cervical spine is more complete with SB-BSCTA compared with PR-BSCTA (*C* and *D*). The OA (*arrow*) can be identified with both approaches. The right ECA is occluded.

cervical internal carotid artery [ICA], external carotid artery [ECA], vertebral artery [VA], basilar artery [BA], petrocavernous ICA [PC-ICA], and ophthalmic artery [OA]) was rated by using the following image-quality scoring system: 1 = vessel not visible; 2 = vessel partly visible, large bone remnants; 3 = vessel visible, bone remnants >1-cm maximal diameter; 4 = vessel clearly visible, bone remnants <1-cm maximal diameter; 5 = vessel clearly visible, no or irrelevant bone remnants. The presence of subtraction artifacts was evaluated separately; the nonsubtracted CTA dataset served as a reference for this purpose.

To examine the relationship between image quality and patient motion, we then performed a quantitative analysis of the amount of motion between the 2 scans. For this step, an image-fusion software tool was used in which both datasets were projected on top of each other and displacement of bone could be measured in 3D. For each patient, the maximal amplitude of displacement for 5 anatomic regions (skull base, upper spine, lower spine, jaw, and hyoid bone) was measured; the precision of the digital ruler applied was 0.1 mm. These measurements were performed by 2 experienced readers in consensus.

Statistical Analysis

The image-quality scores for the 3 algorithms were ranked and plotted as mean ± SD, median, and range. The significance of differences was tested by using the Wilcoxon signed rank test. A 2-sided value of $P < .05$ was considered significant. The kappa statistic was used to assess the level of observer agreement on image quality achieved by the 3 methods. A value of <0.20 implied poor agreement; 0.21–0.40, fair agreement; 0.41–0.60, moderate agreement; 0.61–0.80, substantial agreement; and 0.81–1.0, almost perfect agreement.[18] The mean and SD of the measurements for bone displacement between the scans were calculated. We considered the SD as a measure for the complexity of motion and analyzed its influence

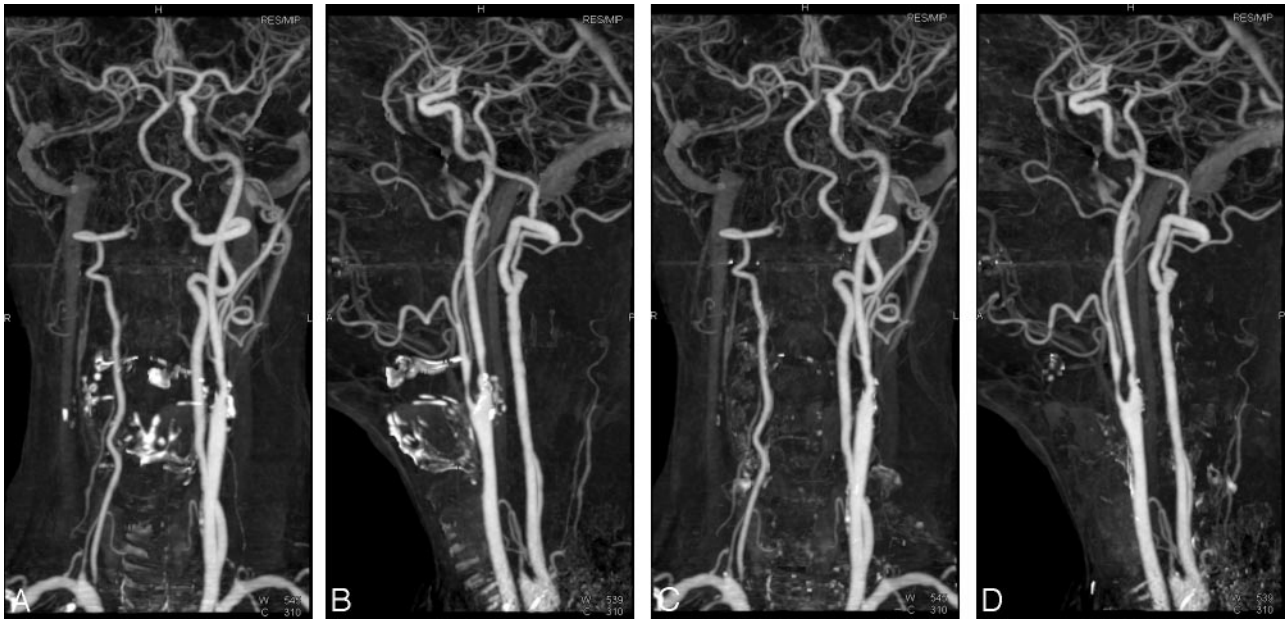

Fig 3. CTA (MIP, frontal [*A* and *C*] and lateral [*B* and *D*] views) shows a patient with occlusion of the right carotid artery and steno-occlusive disease at the left carotid bifurcation and right VA. Both registration techniques provide excellent image quality; more bone remnants can be depicted with SB-BSCTA (*A* and *B*) in comparison with PR-BSCTA (*C* and *D*) in this patient.

Table 2: Influence of the 3 registration procedures on image quality of different vessels (*P* values, Wilcoxon test)*

	Reader 1			Reader 2		
Vessel	BSCTA vs SB-BSCTA	BSCTA vs PR-BSCTA	SB-BSCTA vs PR-BSCTA	BSCTA vs SB-BSCTA	BSCTA vs PR-BSCTA	SB-BSCTA vs PR-BSCTA
CCA	.000	.000	.353	.000	.000	.052
ICA	.000	.000	.003	.000	.000	.001
ECA	.000	.000	.000	.002	.000	.000
PC-ICA	.001	.007	.180	.050	.104	.564
VA	.000	.000	.870	.000	.000	.108
BA	.103	.180	.564	.414	.103	.157
OA	.317	.564	1.0	.317	.157	.317

* Differences between bone subtraction without and with motion compensation are statistically significant for all vessels except for the BAs and OAs; differences between SB- and PR-BSCTA are statistically significant for the ECA and the cervical ICA.

Table 3: Interobserver agreement for the assessment of the vascular segments with 3 registration algorithms*

	BSCTA	SB-BSCTA	PR-BSCTA
CCA	0.95	0.73	0.80
ICA	0.97	0.91	0.93
ECA	0.95	0.81	0.72
PC-ICA	0.87	0.52	0.60
VA	0.98	0.82	0.69
BA	0.90	0.64	0.46
OA	0.68	0.67	0.70

* The kappa values indicate high overall interobserver agreement for the assessment of the different vascular segments.

on image quality for each of the bone-subtraction algorithms by using the Spearman correlation. All calculations were performed by using STATA 8.0 (StataCorp, College Station, Tex).

Results

The study population consisted of 41 male and 13 female patients; mean age was 60.5 ± 9.4 years (range, 29–85 years). The atherosclerosis group had 24 patients, and the oncology group had 30 patients. All examinations were performed without complications or technical problems. BSCTA was technically feasible, with NECT scans and late venous scans to create a bone mask. Reconstruction time was 3 minutes on average for BSCTA without motion compensation and 7 minutes on average for BSCTA with motion compensation (SB-BSCTA, PR-BSCTA) for datasets with an average of 384 images per scan (2 × 384 = 768 images per patient).

Mean enhancement values measured in the CCA were 379 ± 85 HU (range, 220–620 HU) in subtraction images with NECT and 358 ± 82 HU (range, 240–520 HU) in subtraction images with late venous phase scans for bone masking.

Basic restraining measures were applied, namely fixation in a standard CT head holder device with a single strap. The patients were allowed to breathe freely during the examination but were asked to avoid swallowing. The time interval between the 2 scans was 25 seconds for group 1 and 80 seconds for group 2 on average. Mean displacement of bony structures between the 2 scans (mask and CTA) was lowest for the spine (lower spine, 1.3 ± 0.7 mm; upper spine, 1.4 ± 0.8 mm) and highest for the jaw (2.2 ± 1.3 mm) and hyoid (2.3 ± 1.1 mm); the mean displacement of the skull base was 1.6 ± 0.9 mm.

Although high scores for image quality were found for each method, algorithms with motion compensation were able to improve subtraction quality. This improvement was most evident in datasets with interscan motion (Fig 1). The mean scores for image quality were higher with SB- (4.31) and PR-BSCTA (4.43) compared with BSCTA (3.88). A summary of the quality scores for the individual vascular territories is given in Table 1. Image quality differed significantly ($P < .001$ to $P = .007$) between BSCTA and

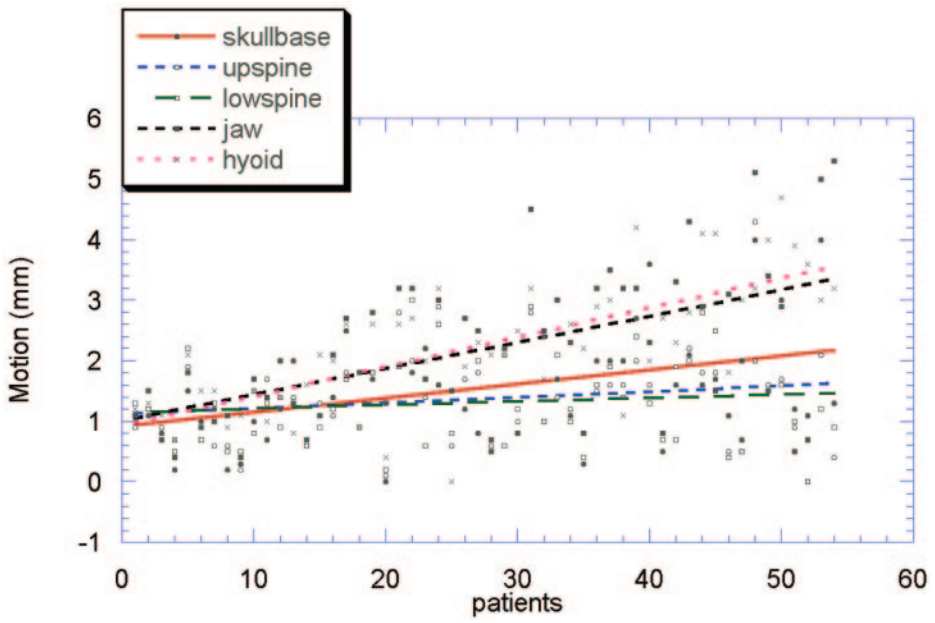

Fig 4. Graphic representation of the individual motion amplitudes for each patient. Note that the patients are ranked by increasing complexity of motion. Trend lines indicate the displacement of different anatomic landmarks.

each of the 2 methods with motion compensation, SB-BSCTA and PR-BSCTA, for all vessels, except the BA and OA. Image quality between SB-BSCTA and PR-BSCTA did not differ significantly for the assessment of the CCA ($P = .564$), PC-ICA ($P = .157$), VA ($P = .286$), BA ($P = .655$), and OA ($P = .414$), but PR-BSCTA was rated superior to SB-BSCTA for the evaluation of the ICA ($P < .001$) and ECA ($P < .001$) (Figs 1–3). The individual results are given in Table 2.

Cohen kappa test revealed a high level of interobserver agreement (BSCTA, $\kappa = 0.68–0.98$; SB-BSCTA, $\kappa = 0.64–0.91$; PR-BSCTA, $\kappa = 0.46–0.93$) for image-quality scores (Table 3).

The lowest scores for image quality were depicted for the delineation of the vertebral artery. The mean values were 2.51 (BSCTA), 3.56 (SB-BSCTA), and 3.62 (PR-BSCTA). Although motion compensation could substantially improve image quality, incomplete removal of the cervical vertebrae, the hyoid bone, and thyroid cartilage (Fig 1) still led to impaired visualization (score 1–3) of the vertebral arteries in 46%/48% (examiner 1/examiner 2) of cases with SB-BSCTA and 41%/37% of cases with PR-BSCTA.

Motion amplitudes for the 5 anatomic landmarks are plotted for each patient in Fig 4. In this plot, the patients were ordered by the SD of their motion amplitudes. Trend lines indicate the overall displacement of the skull base, upper and lower cervical spine, jaw, and hyoid between the 2 scans. A statistically significant inverse relation between image quality and the complexity of motion, expressed by the SD of the motion amplitudes, was found for both the VA and the cervical ICA for all 3 methods ($P = .008–.044$, Spearman correlation). The null hypothesis of independence between image quality and SD of motion could not be rejected for the PC-ICA ($P = .07–.23$, Spearman correlation). The regression lines for the different methods and vascular segments are given in Fig 5*A–C*.

The OA could be visualized bilaterally without interruption in 44% and unilaterally without interruption in another 23% (Fig 2). In the remainder of the patients, a short segment of the OA within the optic canal was not visualized. Vessel irregularities up to short-segment interruptions of the OAs, at least partially related to the subtraction process, were seen in 88% of patients. Misregistration errors were encountered with calcified plaques at the carotid bifurcation. In 35% of the patients, calcified plaques were detected, and complete removal of the calcifications could not be achieved with either method (Figs 2 and 3).

Discussion

CTA is increasingly used in the evaluation of intra- and extracranial vasculature, particularly in the detection and evaluation of intracranial aneurysms and vascular occlusive disease in the neck. To acquire views comparable with digital subtraction angiography, which is considered the standard of reference, one must postprocess CTA data and often perform manual editing to remove bone. This approach has several significant limitations, including an added time demand and the problem of separating bone and contrast-enhanced vessels in areas of close contact between the 2 (ie, at the skull base). Furthermore, the results are highly dependent on the operator's postprocessing skills and are also difficult to standardize. Fully automated procedures, without user interaction, promise a certain degree of standardization and avoid trapping the examiner at the workstation. Especially in the emergency situation, runtime efficiency is a major priority; 5–10 minutes of postprocessing time may be regarded as an upper limit to be clinically useful. In this study, bone-subtraction postprocessing time averaged 3–7 minutes. The added patient radiation dose for the bone-subtraction protocol was 27% (effective dose for NECT scan, 0.65/0.72 mSv [male/female]; effective dose for CTA scan, 2.34/2.61 mSv; scanning range, 200 mm) based on dose estimate performed with WinDose (Institute of Medical Physics, University of Erlangen, Erlangen, Germany).[19]

Motion within the scans or between the nonenhanced and contrast-enhanced scans is a major problem for subtraction procedures. All possible measures should be taken to minimize patient motion; these include detailed patient instruction, comfortable fixation of the patient on the examination table, and optimization of the examination protocol. The application of special external restraining devices like stereotactic frames,[20] external frames with a mouthpiece, as well as vacuum cushions[21] have been proposed to improve patient fixation. To minimize the interscan delay, we performed the circulation time measurements before obtaining the nonenhanced scan. The nonenhanced scan was immediately followed by the contrast-enhanced scan, with the appropriate individual scan delay for contrast arrival after a short patient notification. To test the performance of the algorithms, we specifically included a second patient group, in whom late venous scans were used to create a bone mask, assuming an

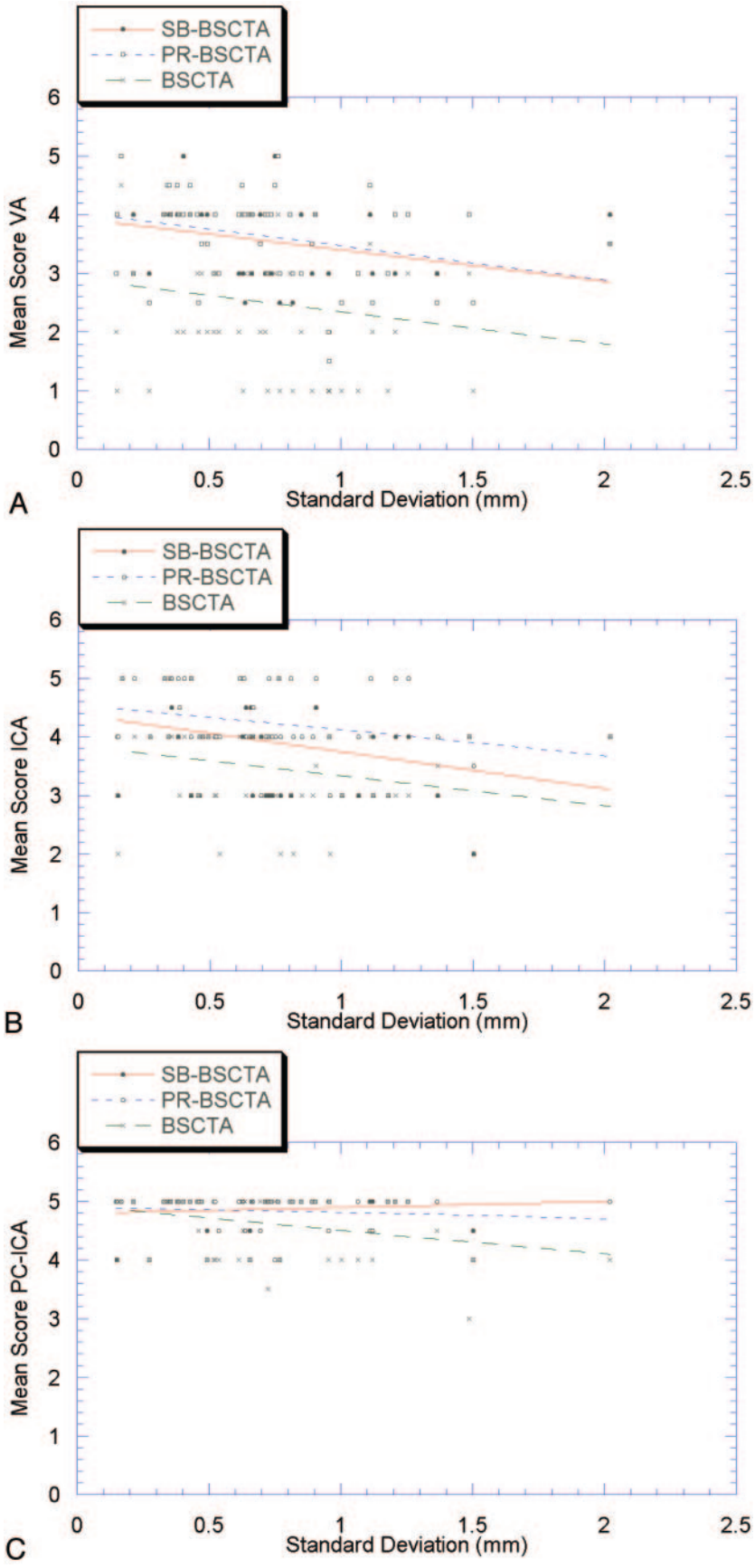

Fig 5. Graphic representation (and trend lines) of the quality scores achieved with the different techniques for individual vessels (*A,* VA. *B,* Cervical ICA. *C,* PC-ICA). There is a trend toward decreased image quality with increasing complexity of motion, expressed by the SD of the motion amplitudes except for the PC-ICA.

increase of interscan motion due to the extended delay between the 2 scans.

Although motion between the 2 scans can be sufficiently compensated with bone mask approaches for the intracranial compartment,[10,12] this is not the same in the neck. Here complex movements between different bones (eg, skull, mandible, and vertebrae) occur. This is reflected in our data, in which the highest image-quality scores were found for arteries located near the skull base, where motion between individual bones is minimal, and the less favorable scores were found in vessel segments, where a higher degree of freedom of movement is possible. The fact that the amount of connected voxels assigned to bone within a 3D data volume influences the registration procedures helps to account for the observation that bone removal is superior near the skull base and less favorable at distant sites. We found this to be true for all registration algorithms but most pronounced for the pure rigid registration. The SB-BSCTA copes with this problem by registering on subvolumes, whereas the PR-BSCTA algorithm uses iterative registration steps on misregistered areas.

A different strategy was introduced by van Straten et al,[11] who proposed removal of bone by piecewise-matched mask bone elimination: After registration of the CTA and nonenhanced scans, the bone in the CTA scan is masked and the different bones are separated by using a watershed algorithm and then registered individually. The average processing time for this procedure was not reported, but most likely would be beyond 10 minutes. The SB-BSCTA and the PR-BSCTA approach omit the fragile segmentation step, and misregistration is compensated either by subdividing the 3D volume into multiple slabs with individual partial rigid registration. Reconstruction time was 3 minutes on average for BSCTA without motion compensation and 7 minutes on average for BSCTA with motion compensation (SB-BSCTA, PR-BSCTA). The mean image-volume load was 384 images per scan ($2 \times 384 = 768$ images per patient). Because no user interaction is necessary during the calculation process and the CTA dataset is available for evaluation in the meantime, this seems to be an acceptable timeframe, even in the emergency situation.

A remarkable finding was that the type of registration did not alter the depiction of the OA. This artery can serve as a marker to test the performance of a bone-subtraction process because of its small lumen diameter and its tight contact to bone within the optic nerve canal. Global dilation of the bone mask, which is

usually performed to minimize bone remnants after subtraction, can erroneously eliminate this vessel in the final image. To address this problem, we perform a local subtraction without mask dilation at areas of close vessel-bone contact. Although artificial lumen reduction or interruption is not completely related to the subtraction process (the image-reconstruction algorithm [convolution kernel] as well as the voxel size contributes to it), we were able to depict the vessel bilaterally without interruption in 44% and unilaterally without interruption in another 23% of the patients with both SB-BSCTA and PR-BSCTA. SB-BSCTA and PR-BSCTA algorithms were not superior to the pure rigid BSCTA method for the evaluation of the basilar artery. This outcome is likely because the image-quality scores were already high for this vessel, and misregistration of the skull base was minimal with each of the different algorithms described previously.

The aims of our study were to evaluate the ability of 2 novel registration techniques to compensate for patient motion. We evaluated the extent of bone removal by measuring the size of bone remnants and, through a direct comparison of subtracted and unsubtracted CTA studies, searched for possible artifacts introduced by the subtraction processes. Therefore, we did not use conventional x-ray angiography as a standard of reference for the assessment of image quality.

A limitation of the algorithms is their inability to precisely register calcified plaques in the walls of vessels featuring significant pulsation. Therefore, we recommend using bone subtraction to depict and present vascular pathology but suggest that morphologic measurements should always be performed on the original CTA data. An approach that could overcome this problem has been described by Beier er al,[22] who introduced an elastic warping method for (2D) image registration on a section-by-section basis to separate vessels from surrounding bone. Runtime was a major drawback, ranging from 1 to 2 hours per dataset.

Elaborate techniques have been developed to omit an additional scan and extract the vascular information from the CTA scan. Vega Higuera et al[23] proposed a threshold-based approach for the elimination of the skull base by using bidimensional transfer functions for direct volume rendering of aneurysms involving the skull base. In their approach, in addition to voxel intensities, gradient magnitudes were also considered to create the mapping from volume data to colors and opacities. Abrahams et al[24] developed a method for bone-free rendering by using iterative relative fuzzy connectedness of 3D CTA datasets to examine the cerebral vasculature without the intervening cranial base. Their preliminary results showed that bone structures could be removed, and vascular anatomy could be isolated by using an almost completely automated process.

A major limitation of this approach was a run-time of 45–60 minutes per patient. An important additional limitation of the previously mentioned techniques is that the number of subjects studied is very small, making it difficult to extract general recommendations. Our study demonstrated the efficiency of both algorithms in a large patient population. Because the image-quality scores of most vessels were improved through the use of subtraction methods with motion compensation and no scores were diminished, we suggest that the reader consider incorporating such postprocessing methods into clinical practice as they become more widely available, since the time demand for processing seems reasonable.

Conclusion

Our results suggest motion compensation can be achieved satisfactorily in most cases through the implementation of SB-BSCTA and PR-BSCTA. Both algorithms provided high image-quality scores in the neck and brain region with low interobserver variability. In the neck region, registration algorithms with motion compensation were superior to registration without motion compensation. The visualization of the ICA and ECA could be optimized with PR-BSCTA, enhancing the usability of bone subtraction in the neck region.

References

1. Achenbach S, Ropers D, Pohle FK, et al. **Detection of coronary artery stenoses using multi-detector CT with 16 × 0.75 collimation and 375 ms rotation.** *Eur Heart J* 2005;26:1978–86. Epub 2005 May 27
2. Bartlett ES, Walters TD, Symons SP, et al. **Quantification of carotid stenosis on CT angiography.** *AJNR Am J Neuroradiol* 2006;27:13–19
3. Coxson HO, Baile EM, King GG, et al. **Diagnosis of subsegmental pulmonary emboli: a multi-center study using a porcine model.** *J Thorac Imaging* 2005;20:24–31
4. Ghersin E, Litmanovich D, Dragu R, et al. **16-MDCT coronary angiography versus invasive coronary angiography in acute chest pain syndrome: a blinded prospective study.** *AJR Am J Roentgenol* 2006;186:177–84
5. Kanne JP, Lalani TA. **Role of computed tomography and magnetic resonance imaging for deep venous thrombosis and pulmonary embolism.** *Circulation* 2004;10(12 suppl 1):I15–21
6. Leiner T, de Haan MW, Nelemans PJ, et al. **Contemporary imaging techniques for the diagnosis of renal artery stenosis.** *Eur Radiol* 2005;15:2219–29
7. Wermer MJ, van der Schaaf IC, Velthuis BK, et al. **Yield of short-term follow-up CT/MR angiography for small aneurysms detected at screening.** *Stroke* 2006; 37:414–18
8. Kouskouras C, Charitanti A, Giavroglou C, et al. **Intracranial aneurysms: evaluation using CTA and MRA—correlation with DSA and intraoperative findings.** *Neuroradiology* 2004;46:842–50
9. Villablanca JP, Jahan R, Hooshi P, et al. **Detection and characterization of very small cerebral aneurysms by using 2D and 3D helical CT angiography.** *AJNR Am J Neuroradiol* 2002;23:1187–98
10. Lell M, Anders K, Klotz E, et al. **Clinical evaluation of bone-subtraction CT angiography (BSCTA) in head and neck imaging.** *Eur Radiol* 2006;16:889–97
11. van Straten M, Venema HW, Streekstra GJ, et al. **Removal of bone in CT angiography of the cervical arteries by piecewise matched mask bone elimination.** *Med Phys* 2004;31:2924–33
12. Venema HW, Hulsmans FJ, den Heeten GJ. **CT angiography of the circle of Willis and intracranial internal carotid arteries: maximum intensity projection with matched mask bone elimination-feasibility study.** *Radiology* 2001;218:893–98
13. Tomandl BF, Hammen T, Klotz E, et al. **Bone-subtraction CT angiography for the evaluation of intracranial aneurysms.** *AJNR Am J Neuroradiol* 2006;27:55–59
14. Majoie CB, van Straten M, Venema HW, et al. **Multisection CT venography of the dural sinuses and cerebral veins by using matched mask bone elimination.** *AJNR Am J Neuroradiol* 2004;25:787–91
15. Sakamoto S, Kiura Y, Shibukawa M, et al. **Subtracted 3D CT angiography for evaluation of internal carotid artery aneurysms: comparison with conventional digital subtraction angiography.** *AJNR Am J Neuroradiol* 2006;27:1332–37
16. Pluim JP, Maintz JB, Viergever MA. **Mutual-information-based registration of medical images: a survey.** *IEEE Trans Med Imaging* 2003;22:986–1004
17. Urschler M, Ditt H, Bischof H. **Partially rigid bone registration in CT angiography.** Presented at: 11th Computer Vision Winter Workshop 2006, Telc, Czech Republic, February 6–8, 2006
18. Landis JR, Koch GG. **The measurement of observer agreement for categorical data.** *Biometrics* 1977;33:159–74
19. Kalender WA, Schmidt B, Zankl M, et al. **A PC program for estimating organ dose and effective dose values in computed tomography.** *Eur Radiol* 1999;9:555–62
20. Gorzer H, Heimberger K, Schindler E. **Spiral CT angiography with digital subtraction of extra- and intracranial vessels.** *J Comput Assist Tomogr* 1994;18:839–41
21. Jayakrishnan VK, White PM, Aitken D, et al. **Subtraction helical CT angiography of intra- and extracranial vessels: technical considerations and preliminary experience.** *AJNR Am J Neuroradiol* 2003;24:451–55
22. Beier J, Oellinger H, Richter CS, et al. **Registered image subtraction for CT-, MR- and coronary angiography.** *Eur Radiol* 1997;7:82–89
23. Vega Higuera F, Sauber N, Tomandl BF, et al. **Enhanced 3D-visualization of intracranial aneurysms involving the skull base.** In: *Proceedings of Medical Image Computing and Computer Assisted Intervention*. Berlin:Springer;2003:256–62
24. Abrahams JM, Saha PK, Hurst RW, et al. **Three-dimensional bone-free rendering of the cerebral circulation by use of computed tomographic angiography and fuzzy connectedness.** *Neurosurgery* 2002;51:264–68